Serum exosomes mediate delivery of arginase 1 as a novel mechanism for endothelial dysfunction in diabetes

Huina Zhang[a,b,c,d,e,1,2], Jian Liu[c,d,e,1], Dan Qu[c,d,e], Li Wang[c,d,e], Chi Ming Wong[c,d,e], Chi-Wai Lau[c,d,e], Yuhong Huang[c,d,e], Yi Fan Wang[c,d,e], Huihui Huang[f], Yin Xia[f], Li Xiang[g], Zongwei Cai[g], Pingsheng Liu[h], Yongxiang Wei[a,b], Xiaoqiang Yao[c,d,e], Ronald Ching Wan Ma[i], and Yu Huang[c,d,e,2]

[a]Beijing An Zhen Hospital, Capital Medical University, 100029 Beijing, China; [b]Key Laboratory of Upper Airway Dysfunction-related Cardiovascular Diseases, Beijing Institute of Heart Lung and Blood Vessel Disease, 100029 Beijing, China; [c]Shenzhen Research Institute, Chinese University of Hong Kong, Hong Kong, China; [d]Institute of Vascular Medicine, Chinese University of Hong Kong, Hong Kong, China; [e]Li Ka Shing Institute of Health Sciences, Chinese University of Hong Kong, Hong Kong, China; [f]School of Biomedical Sciences, Faculty of Medicine, Chinese University of Hong Kong, Hong Kong, China; [g]State Key Laboratory of Environmental and Biological Analysis, Department of Chemistry, Hong Kong Baptist University, Hong Kong, China; [h]National Laboratory of Biomacromolecules, Institute of Biophysics, Chinese Academy of Sciences, 100101 Beijing, China; and [i]Department of Medicine and Therapeutics, Chinese University of Hong Kong, Hong Kong, China

Edited by Gregg L. Semenza, Johns Hopkins University School of Medicine, Baltimore, MD, and approved June 14, 2018 (received for review December 12, 2017)

Exosomes, abundant in blood, deliver various molecules to recipient cells. Endothelial cells are directly exposed to circulating substances. However, how endothelial cells respond to serum exosomes (SExos) and the implications in diabetes-associated vasculopathy have never been explored. In the present study, we showed that SExos from diabetic *db/db* mice (*db/db* SExos) were taken up by aortic endothelial cells, which severely impaired endothelial function in nondiabetic *db/m*$^{+}$ mice. The exosomal proteins, rather than RNAs, mostly account for *db/db* SExos-induced endothelial dysfunction. Comparative proteomics analysis showed significant increase of arginase 1 in *db/db* SExos. Silence or overexpression of arginase 1 confirmed its essential role in *db/db* SExos-induced endothelial dysfunction. This study is a demonstration that SExos deliver arginase 1 protein to endothelial cells, representing a cellular mechanism during development of diabetic endothelial dysfunction. The results expand the scope of blood-borne substances that monitor vascular homeostasis.

exosome | arginase 1 | endothelium | nitric oxide | diabetes

Exosomes are endosome-derived nanoscale membrane vesicles released into the extracellular fluid compartment via exocytosis (1). Exosomes are secreted by many cell types, including B lymphocytes (2), T lymphocytes (3), epithelial cells (4), tumor cells (5), and hepatocytes (6). A surge of research interest has been recently directed to exosomes because exosomes transport their encircled contents such as proteins, mRNA, and miRNAs to recipient cells via bloodstream, representing a new communication route between cells (7). Through some of these functional molecules, exosomes participate in a broad spectrum of physiological and pathological processes, including immune reaction (2), tumor metastasis (8, 9), neurodegeneration (10), infectious disease (11), and cardiovascular disorder (12). Growing evidence has revealed alterations of exosomal contents, mostly miRNAs, in diabetes and obesity, indicating a pathogenic role of such alterations (13, 14).

The development of cardiovascular complications in diabetes is commonly initiated by endothelial dysfunction, although the underlying mechanisms are still not fully understood. Most studies have primarily emphasized the pathological involvement of cytokines and chemokines, such as angiotensin II (15), oxidized-LDL (16), and advanced glycation end products (17). However, it has never been examined whether tissue-derived exosomes that are present on the order of 10^{10} exosomes/mL in human and rodent blood (12, 18) carry yet-to-be-defined substances to participate in diabetes-related endothelial dysfunction. Endothelial cells are the known recipient cells for exogenous exosomes. Mouse endothelial cells can be stimulated to express endothelial growth factors upon taking up A431 human carcinoma cell-derived exosomes (19). Endothelial cells are in direct and constant contact with autologous serum exosomes (SExos), raising the possibility that endothelial cells upon taking up SExos might evoke a functional response. Therefore, we hypothesize that SExos deliver exosomal molecules to endothelial cells, and SExos are involved in development of endothelial dysfunction in diabetes and obesity.

The present study demonstrates that autologous SExos were able to cross into endothelial cells. We purified and characterized exosomes from the serum of diabetic *db*/*db* mice and observed that these SExos entered endothelial cells of intact aortas and profoundly impaired endothelium-dependent relaxations in aortas of nondiabetic *db*/*m*$^{+}$ mice. Further investigation reveals that exosomal arginase 1 (Arg1, an enzyme that reduces the availability of L-arginine, which is the substrate for eNOS-mediated NO production in endothelium) was most likely to be

Significance

Endothelial dysfunction plays a crucial role in the development of diabetic vasculopathy, but the mechanisms are not fully understood. In this study, we have revealed a previously undefined importance of serum exosomes in regulating endothelial function and vascular homeostasis in diabetes. Through comparative proteomics analysis, arginase1 was found enriched in diabetic serum exosomes and can be transferred to endothelial cells to inhibit NO production, thus impairing endothelial function. This is a cell-to-cell communication mechanism first identified to contribute to vascular dysfunction in diabetes.

Author contributions: H.Z., J.L., and Yu Huang designed research; H.Z., J.L., D.Q., L.W., C.M.W., C.-W.L., Yuhong Huang, Y.F.W., H.H., L.X., and R.C.W.M. performed research; H.Z., J.L., D.Q., L.W., C.M.W., C.-W.L., Yuhong Huang, Y.F.W., H.H., Y.X., L.X., Z.C., P.L., Y.W., and X.Y. analyzed data; and H.Z., J.L., Y.X., and Yu Huang wrote the paper.

The authors declare no conflict of interest.

This article is a PNAS Direct Submission.

Data deposition: The proteomics original data named "mouse serum exosome proteomics" have been deposited to ProteomeXchange via the PRIDE database (accession no. PXD009221).

[1]H.Z. and J.L. contributed equally to this work.

[2]To whom correspondence may be addressed. Email: whinnerzhn@126.com and yu-huang@cuhk.edu.hk.

This article contains supporting information online at www.pnas.org/lookup/suppl/doi:10.1073/pnas.1721521115/-/DCSupplemental.

Published online July 2, 2018.

the mediator, as the vaso-harmful effect of *db*/*db* SExos was markedly diminished following Arg1 silencing. The present study unravels a cellular mechanism by which diabetic mouse SExos induce endothelial dysfunction through delivering exosomal Arg1 to reduce NO bioavailability in endothelial cells in obese and diabetic mice.

Results

Characterization of SExos and Their Incorporation into Endothelial Cells of *db/m*$^+$ Mouse Aortas. SExos from *db*/*m*$^+$ mice were isolated from serum by ultracentrifugation and visualized by transmission electron microscopy after negative staining. Most of the SExos appeared intact with diameters less than 100 nm (Fig. 1*A*), consistent with the proposed size for exosomes (40–100 nm in diameter) (20). To characterize the properties of SExos, real-time assessment was performed by Delta Nano C particle analyzer (Beckman–Coulter). The size of SExos was 75.0 ± 37.9 nm (mean ± SD) (Fig. 1*B*). Western-blotting analysis showed intense CD63 and CD81 (exosome markers) signals in the exosomal fraction but not in the whole serum or in the supernatant without exosomes (Fig. 1*C*). Moreover, 77.5% SExo proteins identified by mass spectrum were recorded in ExoCarta protein database (*SI Appendix*, Table S1), suggesting a high purity of the isolated SExos. Immunofluorescence results showed that PKH67-stained *db*/*m*$^+$ mouse SExos were incorporated into mouse aortic endothelial cells, which increased with prolonged incubation time (Fig. 1*D*). It is reported that such incorporation always occurs through forming multivesicular endosomes (21), and indeed we observed that SExos colocalized with intracellular endosome marker Rab5 in primary mouse aortic endothelial cells (*SI Appendix*, Fig. S1), indicating that SExos are likely to have entered endothelial cell rather than simple adhesion to the cell surface.

SExos from Diabetic Mice Impaired Endothelial Function in Nondiabetic Mouse Conduit and Resistance Arteries. First, we determined the concentration of SExos from *db*/*db* mice and diabetic patients together with their metabolic indexes (*SI Appendix*, Fig. S2 and Table S2). The concentration of SExos from *db*/*db* mice or diabetic patients was higher compared with respective nondiabetic controls (Fig. 2 *A* and *B*). Forty-eight-hour incubation of *db*/*m*$^+$ mouse

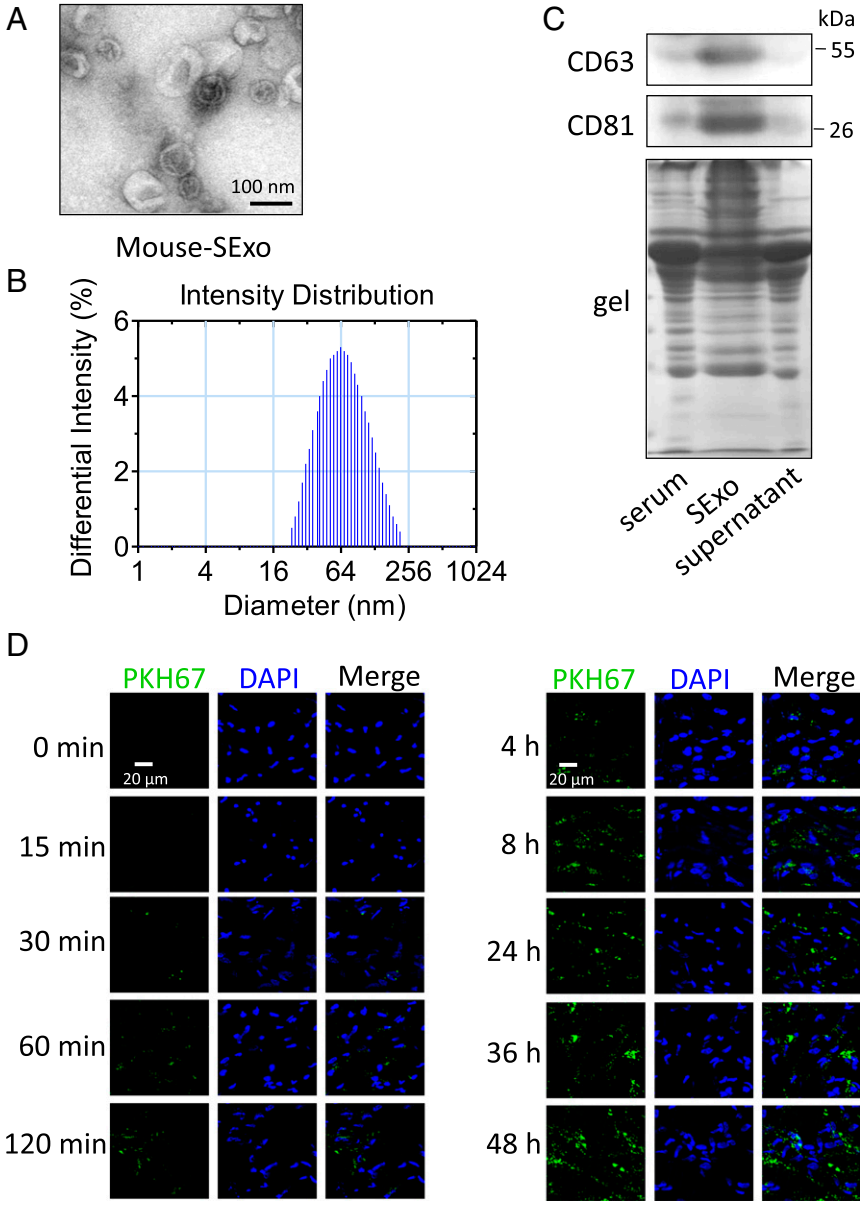

Fig. 1. SExos isolated from *db*/*m*$^+$ serum and absorbed by aortic endothelial cells. (*A*) Electron microscopic image of whole-mounted exosomes purified from *db*/*m*$^+$ SExo. (Bar,100 nm.) (*B*) The size of SExos was analyzed by Delta Nano C particle analyzer. (*C*) Different serum protein fractions were processed for Western-blotting assay with indicated exosome marker antibodies against CD63 and CD81. Silver staining showed the protein-loading amount and protein profile of each sample. (*D*) The *en face* confocal microscopic images showed uptake of SExos by *db*/*m*$^+$ mouse aortic endothelial cells in a time-dependent manner. Nuclei stained by DAPI in blue and SExos stained by PKH67 in green. (Bar, 20 μm.)

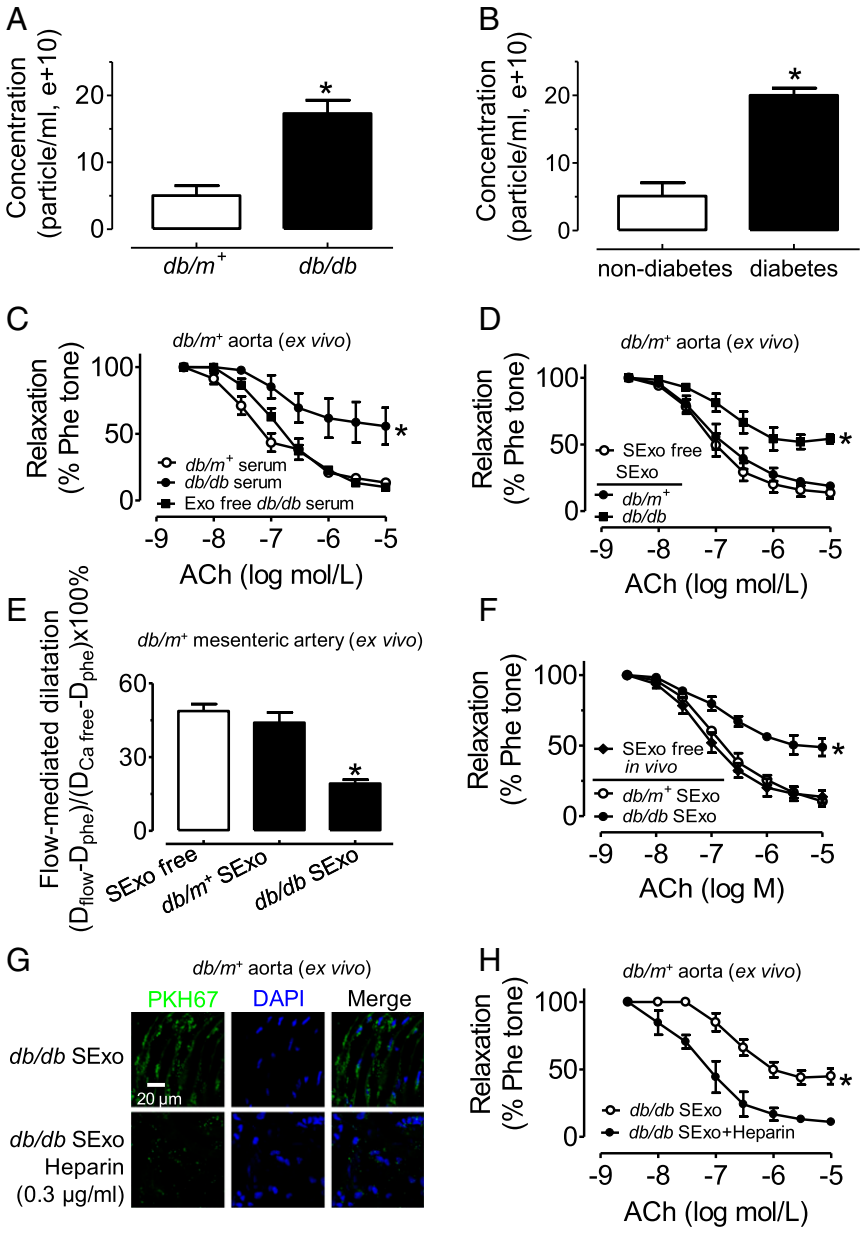

Fig. 2. *db/db* mouse SExos impaired endothelial function in *db/m*$^+$ mouse arteries. (*A*) The number of serum exosomes was higher in *db/db* mouse than *db/m*$^+$ mouse. (*B*) The number of serum exosomes was higher in diabetic patients than nondiabetic subjects. Results are means ± SEM ($n = 4$). *$P < 0.05$ vs. *db/m*$^+$ (*A*) or nondiabetes (*B*). (*C*) *db/db* serum-attenuated acetylcholine (ACh)-induced endothelium-dependent relaxations (EDRs) in *db/m*$^+$ mouse aortas (serum from 1 mL of blood was diluted in serum-free DMEM to a final volume of 1 mL, 48-h treatment), and this effect was absent after removal of Exos from the serum. ACh concentration–response curves (*D*) showed the impaired EDRs in *db/m*$^+$ mouse aortas treated with *db/db* SExos for 48 h. (Exosomes from 1 mL of blood were diluted in 1 mL exosome-free culture medium.) (*E*) Exposure (48 h) to *db/db* mouse SExos reduced flow-mediated dilatation in *db/m*$^+$ mouse mesenteric arteries. (*F*) EDRs in the aortas of *db/m*$^+$ mice were impaired 2 d after tail vein injection of *db/db* SExos. (*G*) Heparin (0.3 μg/mL, 48 h) inhibited the uptake of *db/db* SExos by *db/m*$^+$ mouse aortic endothelial cells. Nuclei stained with DAPI in blue and SExo stained with PKH67 in green. (Bar, 20 μm.) (*H*) Heparin (0.3 μg/mL, 48 h) ameliorated endothelial dysfunction induced by *db/db* SExos. Results are means ± SEM ($n = 4$–5). *$P < 0.05$ vs. *db/m*$^+$ (*A*), nondiabetes (*B*), *db/m*$^+$ serum (*C*), *db/m*$^+$ mouse SExo (*E* and *F*), or *db/db* mouse SExo (*H*).

aortas with *db/db* mouse serum (serum from 1 mL of blood added with exosome-free DMEM to make up a final volume of 1 mL) severely inhibited acetylcholine-induced endothelium-dependent relaxations (EDRs), whereas exosome-free serum did not produce such harmful effects (Fig. 2*C*), suggesting that exosomes from *db/db* mouse serum can impair endothelial function. Indeed, exposure of *db/m*$^+$ mouse aortas to *db/db* SExos (exosomes prepared from 1 mL of blood suspended in 1 mL of exosome-free culture medium) attenuated EDRs (Fig. 2*D*) in both time- and dosage-dependent manner (*SI Appendix*, Fig. S3 *A–D*). Likewise, *db/db* SExos also impaired flow-mediated dilatation (FMD) in resistance mesenteric arteries from *db/m*$^+$ mice (Fig. 2*E* and *SI Appendix*, Fig. S3 *E–G*). By contrast, SExos from *db/m*$^+$ mice did not affect EDRs or FMD in *db/m*$^+$ mouse arteries (Fig. 2 *D* and *E*). In addition, SExos from *db/m*$^+$ mice did not affect EDRs in *db/db* mouse aortas (*SI Appendix*, Fig. S3*H*). Next, SExos from *db/m*$^+$ mice or *db/db* mice were injected into *db/m*$^+$mice via tail vein. Two days after injection, the aortas of *db/m*$^+$ mice receiving *db/db* SExos showed impaired EDRs compared with those receiving *db/m*$^+$ SExos (Fig. 2*F*). Importantly, exosomes from diabetic patients, but not healthy subjects, also impaired EDRs in *db/m*$^+$ mouse aortas in a time-dependent manner (*SI Appendix*, Fig. S4). Heparin was reported to block absorption of exosomes by recipient cells (22). Treatment with heparin (0.3 μg/mL) inhibited the SExos uptake by endothelial cells (Fig. 2*G*) and reversed *db/db* SExos-impaired EDRs in *db/m*$^+$ mouse aortas (Fig. 2*H*). Taken together, these results clearly indicate that exosomes, or most likely the substances they carried, from diabetic mouse serum impaired endothelial function.

Exosomal Proteins Played a Pivotal Role in *db/db* SExos-Induced Impairment of Endothelial Function. To identify whether proteins or RNAs are responsible for the *db/db* SExos-induced endothelial dysfunction, a series of treatments was designed (Fig. 3*A*). The transmission electron microscopic images showed that intact exosomes were loosened, ruptured, and aggregated following a freeze–thaw cycle procedure (Fig. 3*B*). The results of silver staining showed similar profiles between the following treatments: Boil+RNase and Boil (exosomal proteins were inactivated by 100 °C heating); RNase+Proteinase and Proteinase

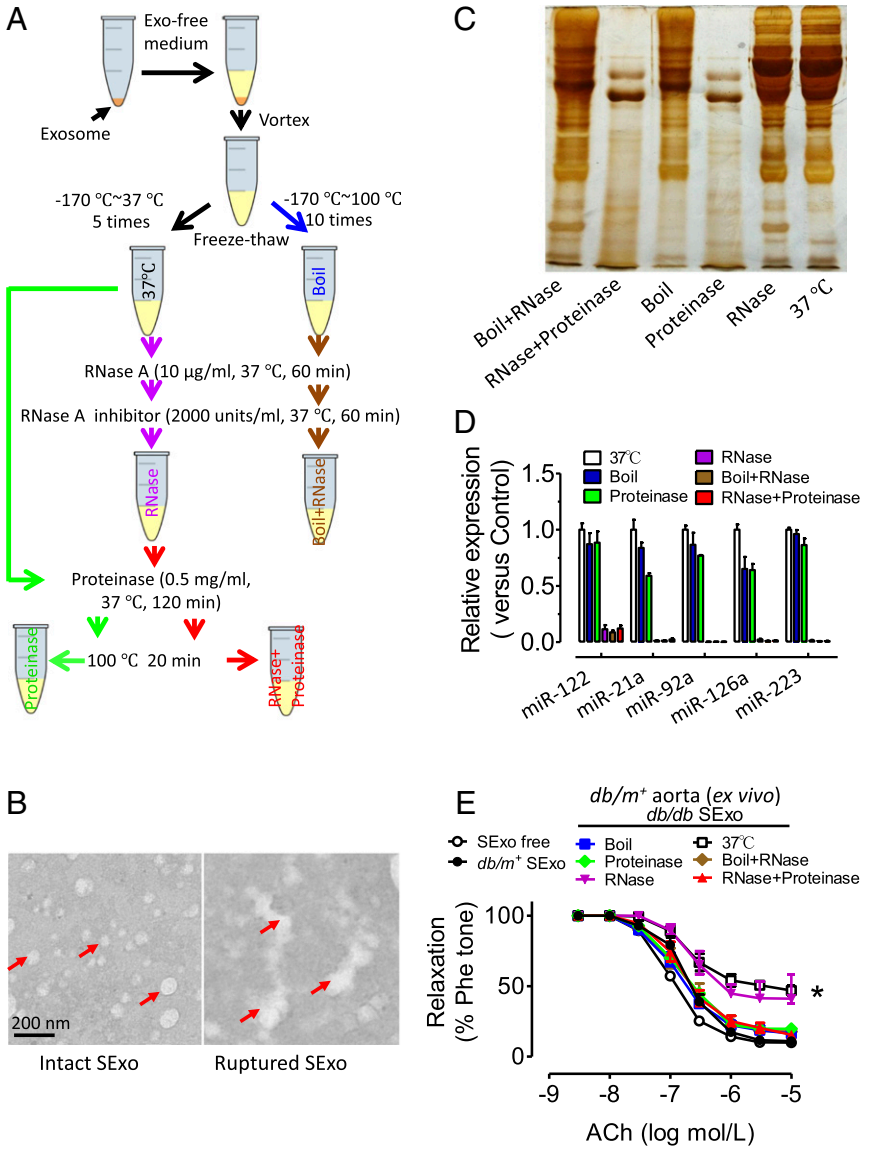

Fig. 3. The exosomal protein played a pivotal role in *db/db* mouse SExo-induced endothelial dysfunction. (*A*) Flowchart illustrated the experimental procedures for removal of proteins or RNAs in *db/db* mouse SExos. (*B*) TEM images showed the *db/db* SExos before (*Left*) and after (*Right*) five freeze–thaw cycles (−170 °C ~ 37 °C). Arrows indicated the intact SExos (*Left*) or ruptured and aggregated SExos (*Right*). (*C*) Silver staining showed the protein profile of *db/db* mouse SExos upon different treatment procedures described in *A*. (*D*) qPCR analysis showed the miRNAs level in *db/db* SExos after different treatments. (*E*) The protein but not RNA fraction in *db/db* SExos caused endothelial dysfunction in *db/m*$^+$ mouse aortas. The 37 °C fraction contains both RNA and proteins; Boil+RNase fraction contains inactivated proteins and trace RNAs; RNase+Proteinase fraction contains trace RNAs and trace proteins; Boil fraction contains RNAs and inactivated proteins; Proteinase fraction contains RNAs and trace proteins; and RNase fraction contains proteins and trace RNAs. Results are means ± SEM ($n = 4$). *$P < 0.05$ vs. *db/m*$^+$ SExo.

(most of the exosomal proteins were degraded by 0.5 mg/mL of proteinase at 37 °C for 120 min); and RNase and 37 °C (intact exosomal protein profile without treatment of 100 °C heating and proteinase) (Fig. 3*C*). Some previously reported exosomal miRNAs were chosen as representatives of the RNA fraction and detected by real-time PCR. The miRNAs in the ruptured SExos were successfully degraded by RNase A (Fig. 3*D*). We next examined which above described preparations retained the ability to impair EDRs in *db/m*$^+$ mouse aortas. The results showed that only the RNase- and 37 °C-treated samples impaired EDRs to a comparable degree as did *db/db* SExos, while the other four preparations (free of active proteins) did not affect EDRs (Fig. 3*E*), suggesting that SExos-induced EDR impairment was most likely attributed to exosomal proteins, but less likely to RNAs. Nevertheless, we cannot completely exclude the possible physiological role of SExo RNAs under the in vivo situation, which may not be recapitulated by the above described ex vivo treatment with different exosomal fractions. In addition, SExo-free medium that underwent various treatments (boiling, RNase A plus RNase A inhibitor or proteinase) did not affect EDRs in *db/m*$^+$ mouse aortas (*SI Appendix*, Fig. S5).

Elevated Arg1 Level in *db/db* Mouse SExos Mediated *db/db* SExo-Induced Endothelial Dysfunction and Exosomal Arg1 Reduced NO Production in Endothelial Cells. To identify the responsible protein(s), we performed a comparative proteomics analysis. Twenty-eight proteins were found to be altered in *db/db* SExos compared with *db/m*$^+$ SExos, with 17 proteins down-regulated and 11 proteins up-regulated (*SI Appendix*, Table S3). Consistently, Western-blotting results showed that the levels of arginase 1 (Arg1), apolipoprotein A-II, and apolipoprotein C-III were elevated, whereas the amount of clusterin was reduced in *db/db* SExos compared with *db/m*$^+$ SExos (Fig. 4*A* and *SI Appendix*, Fig. S6 *A–D*). Of note, SExos Arg1 in diabetic patients was also higher than that in healthy subjects (Fig. 4*B* and *SI Appendix*, Fig. S6*F*), whereas the level of CD63 was similar between the two groups (Fig. 4 *A* and *B* and *SI Appendix*, Fig. S6 *E* and *G*). Western blotting also showed that Arg1 was mainly enriched in SExos rather than other components of serum (*SI Appendix*, Fig. S7), and the levels of Arg1 in *db/db* serum and SExos were significantly higher than those in *db/m*$^+$ serum and SExos, respectively (*SI Appendix*, Fig. S7 *A–C*). Furthermore, Arg1 activity was significantly higher in *db/db* SExos compared with *db/m*$^+$ SExos (Fig. 4*C*). Arginase converts arginine to ornithine and thereby decreases NO production (23) and affects endothelial function (24–28). Hence, exosomal Arg1 was selected

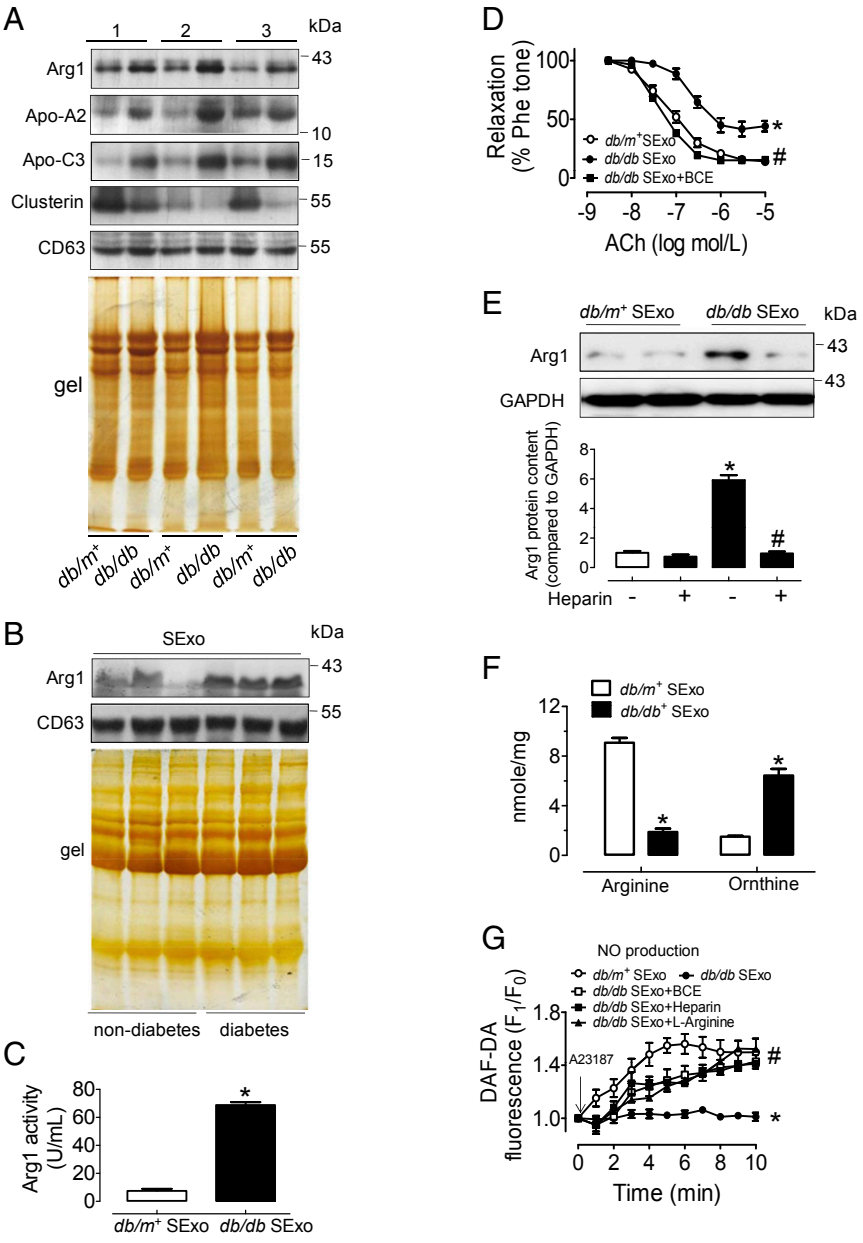

Fig. 4. Arg1 increased in diabetic mouse SExos and participated in *db/db* SExo-impaired endothelial function. (*A*) After iTRAQ quantification, some of the identified SExo proteins including Arg1 (Arg1), apolipoprotein A2 (Apo-A2), apolipoprotein C3 (Apo-C3), clusterin, and CD63 were detected in SExos from *db/m*$^+$ and *db/db* mice by Western blotting. Silver staining indicated the amount of protein loading. (*B*) SExos were isolated from healthy subjects and diabetic patients, and Western blotting was carried out to confirm the expression of Arg1 and CD63. Silver staining indicated the protein-loading amount. (*C*) The activity of Arg1 was higher in SExos from the same volume of *db/db* serum compared with those from *db/m*$^+$ serum. (*D*) Treatment for 24 h with BCE (100 μmol/L, arginase inhibitor) added after 24-h exposure to *db/db* SExos restored EDRs in *db/m*$^+$ mouse aortas. (*E*) *db/db* SExos treatment raised the protein level of Arg1 in HUVECs, which was reversed by 24-h treatment with heparin (0.3 μg/mL). (*F*) Arginine and ornithine levels in endothelial cells (H5V cells) after 48-h *db/db* SExos treatment. (*G*) The reduced NO production in *db/db* SExos-treated HUVECs (48 h) was normalized by cotreatment of heparin (0.3 μg/mL, 48 h), BCE (100 μmol/L, 24 h), or L-arginine (300 μmol/L, 24 h). Results are means ± SEM ($n = 3$–6). *$P < 0.05$ vs. *db/m*$^+$ SExo; #$P < 0.05$ vs. *db/db* SExo.

as our target molecule for further investigation. We found that *db/db* SExos-induced impairment of EDRs was inhibited by arginase inhibitor S-(2-boronoethyl)-l-cysteine (BCE, 100 μmol/L) (Fig. 4*D*), suggesting that the exosomal source of Arg1 is most likely to mediate *db/db* SExos-induced endothelial dysfunction. Meanwhile, BCE alone (100 μmol/L, 24 h) did not affect EDRs in *db/m*$^+$ mouse aortas (*SI Appendix*, Fig. S8). Next, we prepared the Arg1-overexpressing adeno-associated virus (AAV) construct (Arg1 OE) (*SI Appendix*, Fig. S9*A*). Ex vivo 48-h transduction of Arg1 OE dose-dependently reduced EDRs in *db/m*$^+$ mouse aortas (*SI Appendix*, Fig. S10*A*), and this effect was reversed by BCE (100 μmol/L, added 24 h after transduction) (*SI Appendix*, Fig. S10*B*). Moreover, Arg1 overexpression suppressed A23187-stimulated NO generation in human umbilical vein endothelial cells (HUVECs), and these effects were reversed by cotreatment with BCE or L-arginine (300 μmol/L, the substrate for both nitric oxide synthase and arginases) (*SI Appendix*, Figs. S10*C* and S11*A*).

Twenty-four-hour treatment with *db/db* SExos increased Arg1 protein content in HUVECs, which was inhibited by heparin (Fig. 4*E*). However, Arg1 mRNA was not changed by exosome treatment (*SI Appendix*, Fig. S10*D*). Furthermore, arginine concentration in *db/db* SExos-treated endothelial cells was significantly decreased, while ornithine concentration was increased correspondingly (Fig. 4*F*). These results suggest that Arg1 plays a functional role upon being taken up by endothelial cells. Consistently, *db/db* SExos exposure (48 h) suppressed A23187-stimulated NO generation in HUVECs, which were reversed by cotreatment with BCE, L-arginine (300 μmol/L), or heparin (0.3 μg/mL) (Fig. 4*G* and *SI Appendix*, Fig. S11*B*).

Exosomes Were the Major Source for the Elevated Arg1 Content in *db/db* Mouse Endothelial Cells. Arg1 signal was more intense in *db/db* mouse endothelium compared with the barely visible signal in *db/m*$^+$ mouse endothelium as shown by *en face* immunofluorescence staining (Fig. 5*A*), whereas arginase 2 (Arg2) was equally expressed (*SI Appendix*, Fig. S12*A*). Next, qPCR analysis showed that Arg1 mRNA was extremely low in endothelial cells isolated from both *db/db* and *db/m*$^+$ mouse aortas (Fig. 5*B*). The identity of endothelial cells was confirmed by the high mRNA level of the

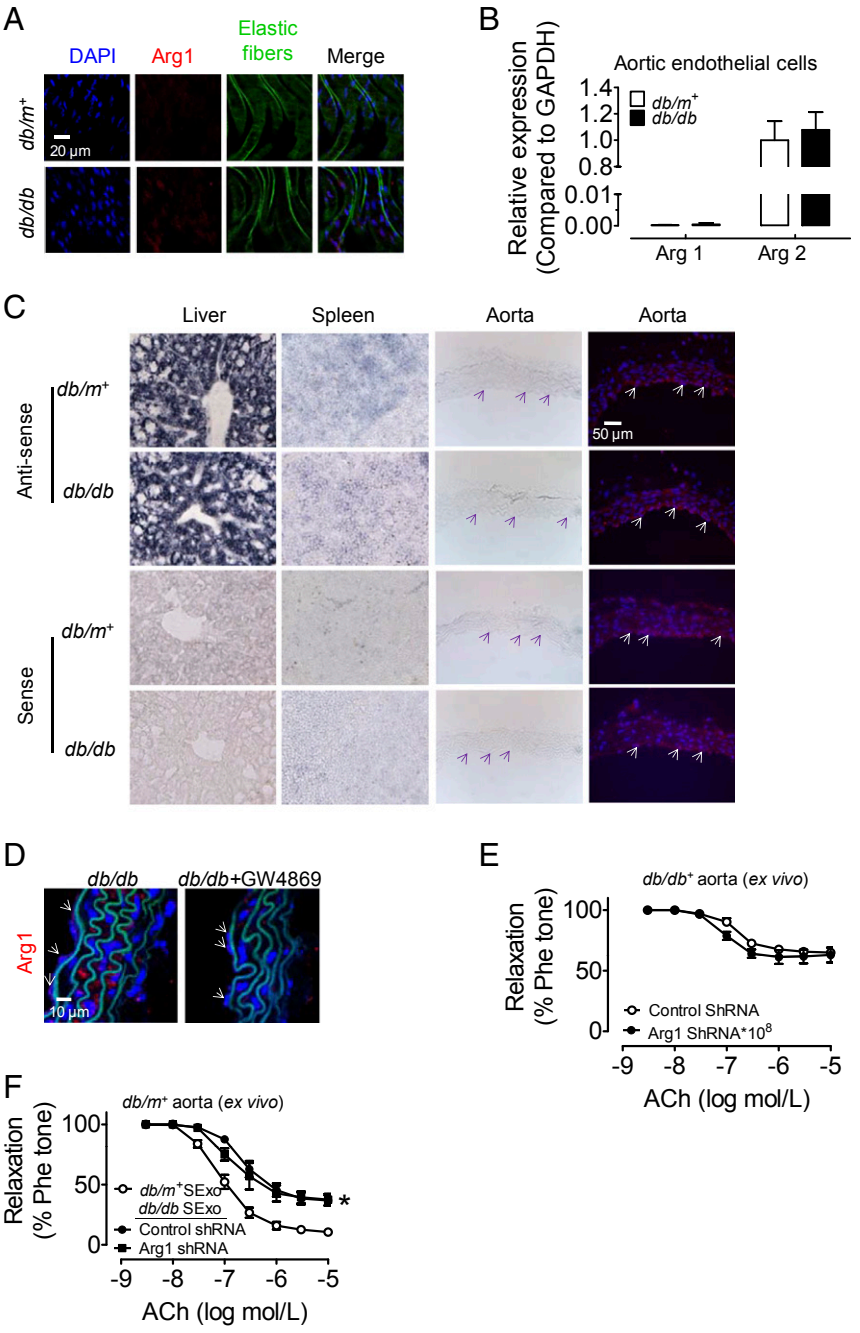

Fig. 5. Arg1 protein content and mRNA expression in endothelial cells of *db/m*$^+$ and *db/db* mouse aortas. (*A*) *En face* immunofluorescence images showed the Arg1 protein level in *db/m*$^+$ and *db/db* mouse aortic endothelial cells. Nuclei stained with DAPI in blue and Arg1 signal stained with TRITC in red; autofluorescence of elastic fibers in green. (Bar, 20 μm.) (*B*) qPCR analysis showed the mRNA expression levels of Arg1 and Arg2 in *db/m*$^+$ and *db/db* mouse aortic endothelial cells. (*C*) Endogenous Arg1 expression in *db/db* or *db/m*$^+$ liver, spleen, and aorta detected by in situ hybridization. The endogenous mRNA expression level of Arg1 was determined using antisense probe and indicated by the intensity of blue color. Sense probe of Arg1 mRNA was used as the negative control. The images in the rightmost column were fluorescence images of the aortas. The blue fluorescence indicated the nucleus, and the white arrows pointed the locations of aortic endothelial cells. (Bar, 50 μm.) (*D*) GW4869 (1 mg/kg/d), a well-known agent for preventing exosome release, was intraperitoneally injected into *db/db* mice for 2 wk, and Arg1 in aortic endothelial cells was detected by immunofluorescence. (*Left*) The aorta from *db/db* mice. (*Right*) The aorta from GW4869-treated *db/db* mice. Red, Arg1; blue, nucleus; green, elastic fibers. White arrows pointed the location of endothelial cells. (Bar, 10 μm.) (*E*) Ex vivo knockdown of Arg1 by Arg1 shRNA did not rescue endothelial function in *db/db* mouse aortas. (*F*) Lack of the effect of Arg1 shRNA on *db/db* SExos-induced endothelial dysfunction. Results are means ± SEM ($n = 4$). *$P < 0.05$ vs. *db/m*$^+$ SExos.

endothelial cell marker VE-cadherin and the extremely low mRNA level of the vascular smooth muscle marker α-SMA (*SI Appendix*, Fig. S12*B*). Furthermore, in situ hybridization showed that Arg1 mRNA was undetectable in the endothelium in either *db/m*$^+$ or *db/db* mouse (Fig. 5*C*).

Next, *db/db* mice were treated with neutral sphingomyelinase inhibitor GW4869 (a widely used agent to inhibit exosome release) for 2 wk. As expected, the amount of serum exosomes was reduced significantly (*SI Appendix*, Fig. S13). Intriguingly, endothelial Arg1 protein expression also decreased dramatically (Fig. 5*D*), suggesting that endothelial Arg1 signals are mainly from SExos.

Furthermore, Arg1 shRNA expressing AAV (Arg1 shRNA) (*SI Appendix*, Fig. S9*B*) did not rescue EDRs in *db/db* mouse aortas (Fig. 5*E*). This result further supports the exogenous origin of increased Arg1 in *db/db* mouse endothelium. Otherwise, Arg1 shRNA should improve endothelial function ex vivo if Arg1 were produced in endothelial cells. Similarly, Arg1 shRNA did not improve EDRs in *db/db* SExos-treated *db/m*$^+$ mouse aortas (Fig. 5*F*).

Arg1 Knockdown in Vivo Restored Endothelial Functions in *db/db* Mice. Seven days after tail i.v. administration of Arg1 shRNA (10^8 pfu) to *db/db* mice, the Arg1 protein level was decreased in *db/db* aortic endothelium (*en face* immunofluorescence staining) and liver compared with control shRNA group (Fig. 6*A* and *SI Appendix*, Fig. S15*A*), while Arg2 expression was unaltered (*SI Appendix*, Fig. S15*B*). Vascular functional analysis showed markedly improved EDRs in aortas and FMD in mesenteric arteries (Fig. 6 *B* and *C*) and increased nitrite generation in aortas challenged by 1 μmol/L ACh in Arg1 shRNA-treated *db/db* mice (Fig. 6*D*). In addition, fasting plasma glucose and insulin sensitivity were not affected in these mice (*SI Appendix*, Fig. S15*C*). More importantly, SExos prepared from Arg1 shRNA-treated *db/db* mice have

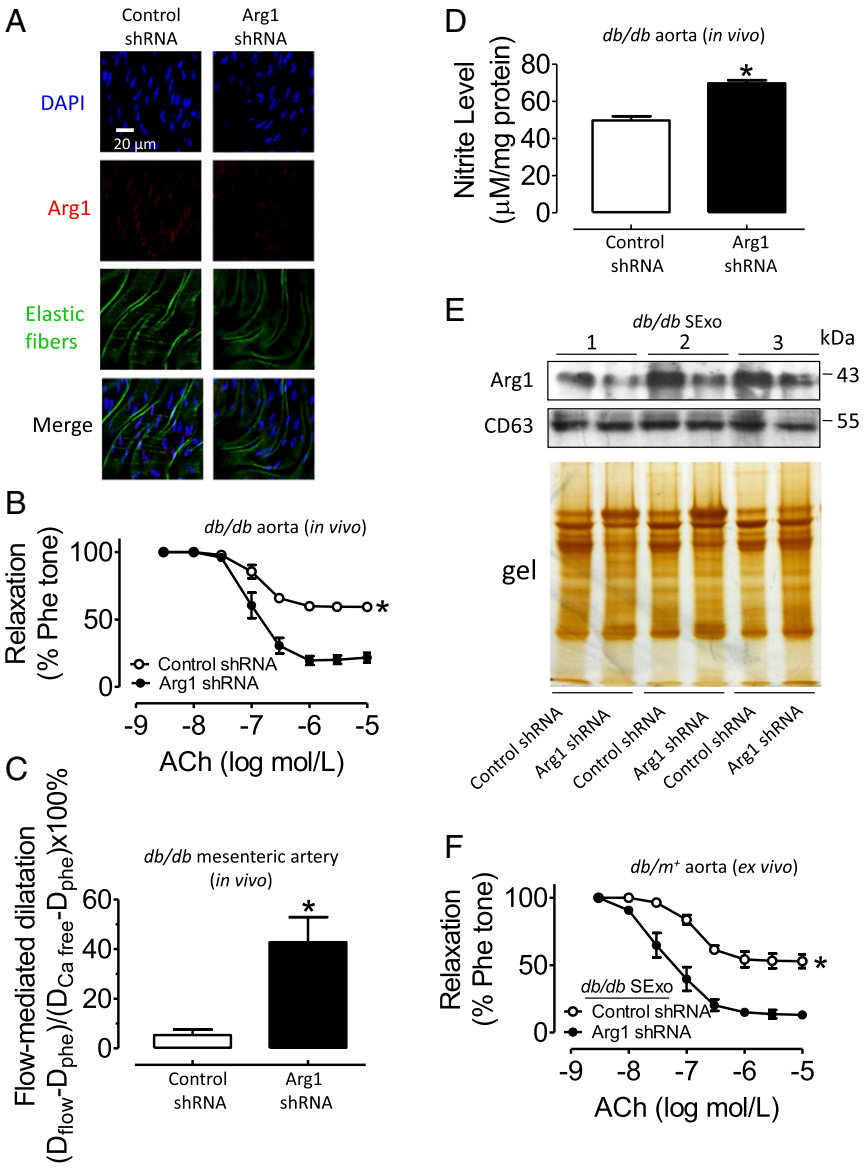

Fig. 6. Knockdown of Arg1 improved EDRs in *db/db* mice. (*A*) The *en face* immunofluorescence images showed the Arg1 protein expression in *db/db* mouse aortic endothelial cells (7 d after tail i.v. injection of Arg1 shRNA to *db/db* mice). Nuclei stained with DAPI in blue, Arg1 signal stained with TRITC in red, and autofluorescence of elastic fibers in green. (Bar, 20 μm.) Arg1 shRNA in vivo improved EDRs in *db/db* mouse aortas (*B*) and flow-mediated dilatation in resistance mesenteric arteries (*C*). (*D*) Arg1 shRNA in vivo increased the nitrite level in *db/db* mouse aortas. (*E*) Arg1 protein expression in SExos from *db/db* mice 7 d after i.v. delivery of control shRNA or AAV-Arg1 shRNA. Silver staining indicated the protein-loading amount. (*F*) SExos isolated from Arg1 shRNA-injected *db/db* mice did not impair EDRs in *db/m*$^+$ mouse aortas after 48-h incubation. Results are means ± SEM ($n = 4$). *$P < 0.05$ vs. control shRNA.

decreased Arg1 protein content (Fig. 6*E* and *SI Appendix*, Fig. S14*A*), and these SExos no longer impaired endothelial function ex vivo in *db/m*$^+$ mouse aortas (Fig. 6*F*), although they were still absorbed by endothelial cells (*SI Appendix*, Fig. S15*D*). It is intriguing to note that the preserved EDRs in the aortas of Arg1 shRNA-treated *db/db* mice were impaired again upon exposure to SExos from nontreated *db/db* mice (*SI Appendix*, Fig. S15*E*). Just like *db/db* SExos, SExos prepared from diet-induced obese (DIO) mice also contained an elevated level of Arg1 (*SI Appendix*, Fig. S16*A*). Again, silencing Arg1 by Arg1 shRNA in vivo reduced serum exosomal Arg1 content and rescued the impaired EDRs in DIO mouse aortas (*SI Appendix*, Fig. S16 *B* and *C*).

In Vivo Arg1 Overexpression Led to Endothelial Dysfunction in *db/m*$^+$ Mice. *En face* immunofluorescence staining showed an increased protein content for Arg1 in SExos and liver 7 d following tail i.v. injection of Arg1 OE (10^8 pfu) to *db/m*$^+$ mice (Fig. 7*A* and *SI Appendix*, Fig. S17*A*). By contrast, the protein expression of Arg2 was not changed in the same preparations (*SI Appendix*, Fig. S17*B*). Arg1 OE attenuated EDRs in *db/m*$^+$ mouse aortas, which was reversed by L-arginine treatment (300 μmol/L) (Fig. 7*B*). In addition, Arg1 OE reduced FMD in *db/m*$^+$ mouse mesenteric arteries (Fig. 7*C*) and lowered the nitrite content in *db/m*$^+$ mouse aortas (Fig. 7*D*). As expected, Western-blotting analysis showed an increased protein content of Arg1 in SExos from Arg1 OE-treated mice (Fig. 7*E* and *SI Appendix*, Fig. S14*B*), and these SExos impaired EDRs in nontreated *db/m*$^+$ mouse aortas after being taken up by endothelial cells; the effects were reduced by the arginase inhibitor BCE (100 μmol/L) or by the exosome absorption inhibitor heparin (0.3 μg/mL) (Fig. 7*F* and *SI Appendix*, Fig. S17*C*). Importantly, myc-tagged Arg1 was detected by *en face* staining in endothelial cells of nontreated *db/m*$^+$ mouse aortas after incubation with SExos isolated from Arg1 OE-treated mice, again demonstrating that exosomal Arg1 was able to be delivered to recipient endothelial cells (*SI Appendix*, Fig. S17*D*).

Discussion

This study highlights the role of serum exosomes as a blood-borne regulator of vascular function and pinpoints Arg1 as a critical exosomal component that participates in endothelial dysfunction in diabetic and obese mice after its delivery to endothelial cells (Fig. 7*G*).

Exosomes are defined as microvesicles of 40–100 nm in diameter. To evaluate the purity of SExos we isolated, a combination of methods was employed, including transmission electron microscopy (TEM), Nano C particle analyzer, mass spectrum, and Western blotting. The size distribution (75.0 ±37.9 nm) and the

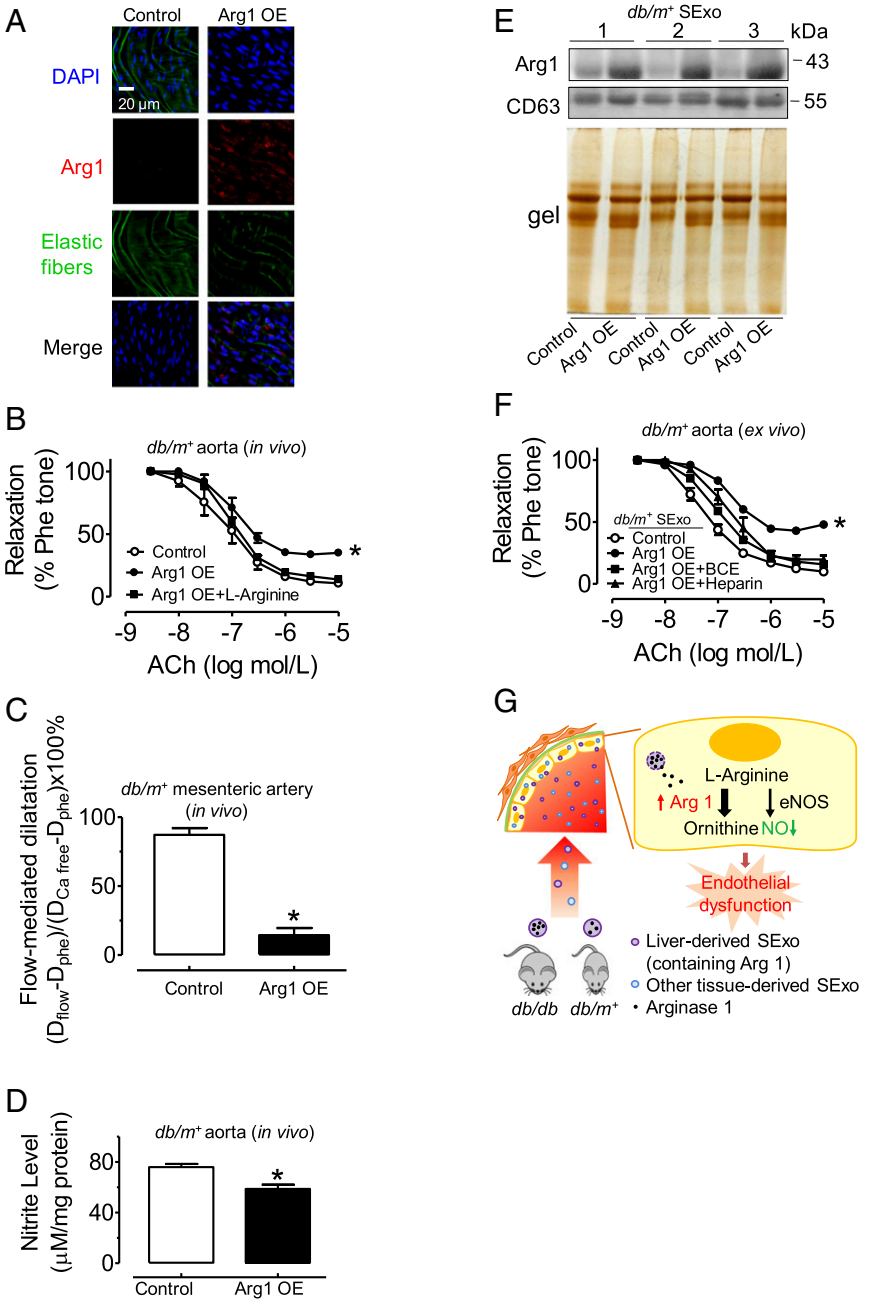

Fig. 7. Overexpression of Arg1 impaired EDRs in *db/m*$^+$ mouse aortas. (*A*) Immunofluorescence images showed the Arg1 protein expression in *db/m*$^+$ mouse aortic endothelial cells (7 d after tail i.v. injection of Arg1 OE to *db/m*$^+$ mice). Nuclei stained with DAPI in blue, Arg1 signal stained with TRITC in red, and autofluorescence of elastic fibers in green. (Bar, 20 μm.) (*B–D*) Arg1 overexpression in vivo reduced EDRs in *db/m*$^+$ mouse aortas, and this effect was reversed by L-arginine (300 μmol/L, 30 min) (*B*), impaired flow-mediated dilatation in resistance mesenteric arteries (*C*), and decreased the nitrite level in aortas (*D*). (*E*) Arg1 protein content in *db/m*$^+$ mouse SExos (7 d after i.v. administration of AAV–control or Arg1 OE). Silver staining indicated the protein-loading amount. (*F*) SExos isolated from Arg1-overexpressed *db/m*$^+$ mice triggered endothelial dysfunction in *db/m*$^+$ mouse aortas after 48-h incubation. Results are means ± SEM ($n = 4$–5). *$P < 0.05$ vs. control. (*G*) The proposed role of SExos in diabetes-associated endothelial dysfunction. *db/db* mouse serum exosomes are absorbed by endothelial cells and subsequently impair endothelium-dependent relaxations through inhibiting NO generation via transfer of exosomal Arg1 (probably delivered mainly from liver) to endothelial cells.

enrichment of the tetraspanins CD63 and CD81 in isolated vesicles concurs with the criteria for defining exosomes (1). About 77.5% of the serum exosomal proteins identified by mass spectrum are documented in the ExoCarta protein database (29), suggesting that the vesicle population we isolated from mouse serum shares exosome-like characteristics.

Exosomes, previously thought to be merely cell debris, have attracted increasing attention in recent years as a novel mechanism for cell-to-cell communication (20). In the present study, autologous SExos isolated from mice were taken up by the mouse aortic endothelium ex vivo in a time-dependent manner. We further demonstrated that *db/db* mouse SExos attenuated EDRs in *db/m*$^+$ mouse aortas. Of note, SExos isolated from diabetic patients also impaired EDRs in *db/m*$^+$ mouse aortas, suggesting that human SExos have a similar property to alter endothelial function as SExos from *db/db* mice.

To identify whether proteins or miRNAs mediate the effect of exosomes, *db*/*db* SExos were treated with proteinase or RNase A to remove proteins or miRNAs, respectively. We observed that only the protein fraction participated in *db*/*db* SExo-induced endothelial dysfunction. The comparative proteomics analysis assisted us to focus on Arg1 among a total of 28 proteins with altered levels in *db*/*db* SExos because arginase is the critical enzyme regulating the turnover of L-arginine, the substrate for endothelial NOS-mediated NO production in endothelial cells. Meanwhile, Arg1 triggers the generation of reactive oxygen species (30). Besides, increased expression and activity of Arg1 were reported in the serum of diabetic patients, implying a potential value of serum Arg1 as a prognostic or diagnostic marker for diabetic vasculopathy (31, 32). More importantly, we found that the Arg1 content in SExos was increased in diabetic patients compared with SExos from healthy subjects. Based on the clinical background and our observations, we hypothesized that exosomal Arg1 contributed to *db*/*db* SExo-induced endothelial dysfunction. We therefore constructed Arg1-silencing virus (Arg1 shRNA) and Arg1-overexpressing virus (Arg1 OE) to validate the critical role of Arg1. First, knocking down Arg1 via in vivo viral transduction lowered the content of serum exosomal Arg1, reduced Arg1 level in native aortic endothelial cells, and restored EDRs in conduit aortas and FMD in resistance arteries in *db*/*db* mice. Importantly, SExos from Arg1 shRNA-transduced *db*/*db* mice no longer impaired endothelial function in *db*/*m*$^+$ mouse aortas. Second, overexpression of Arg1 by Arg1 OE in *db*/*m*$^+$ mice elevated Arg1 levels in both SExos and native endothelial cells and impaired endothelial function in *db*/*m*$^+$ mouse arteries to a similar degree as that in *db*/*db* mouse arteries. Furthermore, similar to *db*/*db* SExos, SExos from Arg1 OE-transduced *db*/*m*$^+$ mice were able to impair EDRs in control mice. Treatment with Arg1 OE or *db*/*db* SExos decreased the capacity of HUVECs to generate NO in response to A23187, and this effect was reversed by cotreatment with either L-arginine or arginase inhibitor BCE.

Previous Western-blotting and immunochemistry analysis showed that Arg1 protein could be detected in vascular endothelium of bovine coronary artery (33) and rat aorta (34), but not in HUVECs (35). Our qPCR results showed little expression of endogenous Arg1 mRNA in HUVECs and MAECs. In contrast, substantial expression of Arg1 mRNA was detected in bovine or porcine endothelial cells and rat aortic endothelial cells (*SI Appendix*, Fig. S18), which is consistent with the previously published data (33–36). These results clearly suggest differential endogenous expression levels of Arg1 in endothelial cells from different species. Our results showed that mRNA expression of endogenous Arg1 was virtually undetectable in mouse aortic endothelial cells by qPCR and in situ hybridization, whereas Arg1 protein was detected by immunofluorescence, suggesting that most of Arg1 protein in endothelial cells is likely to be exogenous at least in mouse endothelial cells. Functional study showed that ex vivo Arg1 shRNA treatment cannot rescue the impaired EDRs in aortas from diabetic mice, whereas SExos from Arg1 shRNA-treated *db*/*db* mice fail to impair EDRs in nondiabetic mouse aortas, further confirming the foreign origin of Arg1 protein detected in mouse endothelial cells. Based on a previous study (37) and our present results (*SI Appendix*, Fig. S19), liver is probably the main tissue that expresses Arg1, and Arg1 can be detected in exosomes secreted by hepatocytes (6). These results indicate that Arg1-containing exosomes are probably mainly from liver, as indicated in a recent report on extracellular vesicles released by cultured rat primary hepatocytes (38). In addition, we also observed a moderate expression of Arg1 in mouse lung and spleen. Unless new reliable methods are developed, it remains difficult to sort out the precise origin(s) of serum exosomal Arg1.

Due to technical constraints, serum proteins, other particles (such as HDL), or protein aggregates may still be present in our exosomal preparations. We cannot exclude the possible involvement of a nonexosomal source of Arg1, albeit to a lesser degree. Because the detailed mechanism underlying secretion and uptake of circulating exosomes is largely unknown, no specific tools are at present available to inhibit exosome release or uptake. Heparin is reported as a general inhibitor for exosome uptake, and here we used heparin to inhibit SExo uptake by endothelial cells in ex vivo and in vitro studies. Nevertheless, new specific interfering tools and more rigorous studies are required to further explore the clinical relevance of SExos in development of diabetic vasculopathy. In addition, the present study cannot discount the possibility that other exosomal proteins with altered levels, such as apolipoprotein C-III, might play a minor role in *db*/*db* SExos-induced impairment of endothelial function, which requires future examination.

In summary, here we report a detailed study revealing that SExos contain functional Arg1 that is deliverable to endothelial cells to inhibit NO production and thus impair endothelial function. We demonstrate that serum exosomal Arg1 is elevated in *db*/*db* mice and in diabetic patients, which is critically involved in endothelial dysfunction under diabetic and obese conditions. The present study unravels, with potential clinical relevance, the previously undefined importance of SExos in the regulation of endothelial function and vascular homeostasis. This novel cell-to-cell communication mechanism may also contribute to vascular dysfunction under various pathogeneses such as hypertension and hyperlipidemia, which warrants further investigation.

Materials and Methods

SI Appendix includes the details of the materials and methods used in the present study.

Experimental Animals. All animal protocols were approved by the Chinese University of Hong Kong Animal Experimentation Ethics Committee and are in compliance with the *Guide for the Care and Use of Laboratory Animals* (39).

Human Blood Samples. The study design was approved by the Chinese University of Hong Kong–New Territories East Cluster Clinical Research Ethics Committee (CREC Ref. No. 2013.304) and by the Beijing Anzhen Hospital Medical Ethics Committee (No. 2017005). Written informed consent was obtained from all participants.

SExos Isolation and Identification. SExos were isolated as reported (40) and assessed by transmission electron microscopy (TEM) and Delsa Nano C particle analyzer (Beckman–Coulter).

Western Blotting. Protein samples were separated on SDS/PAGE, transferred to a PVDF membrane, and then incubated with indicated antibodies and detected by ECL system.

Fluorescent Labeling of SExos and Confocal Microscopy. Mouse SExos were labeled with the fluorescent dye PKH67 (Sigma) and resuspended in exosome free-culture medium in which mouse aortas were submerged. The aortas were hereafter cut open and visualized under confocal microscope (FV1000; Olympus).

Vascular Functional Study. Mouse aortas were dissected out and suspended in wire myograph (Danish Myo Technology) to record isometric force. Second-order resistance mesenteric arteries were cannulated onto pressure myograph to measure flow-mediated dilatation (41).

Detection of mRNAs in Endothelial Cells or microRNAs in SExos. The endothelial cell RNAs were isolated using RNeasy mini kit (QIAGEN), and mRNA expression for VE-cadherin, α-SMA, arginase 1, arginase 2, and GAPDH were detected by qPCR. SExo miRNA was extracted using mirVana miRNA Isolation Kit (Ambion), and miRNA expression levels were determined by Applied Biosystems Taqman miRNA Assay system (42).

Protein Digestion, iTRAQ Labeling, LC-MS/MS Analysis, Protein Identification, and Quantification Analysis. The samples for iTRAQ quantitative analysis were prepared according to the iTRAQ Reagents Protocol (Applied Biosystems). The labeled proteins were analyzed by nanoLC-MS/MS using a Q Exactive equipped with an Easyn-LC 1000 HPLC system (Thermo Scientific). The raw data and protein quantification were analyzed with Proteome Discovery version 1.4. The fold-change threshold for up- or down-regulation was set as mean ± 1.960σ.

AAV Construction. Mouse arginase 1 was PCR-amplified from the pcDNA3.1-mArg1-Flag (a gift from Peter Murray, St. Jude Children's Research Hospital, Memphis, TN, Addgene plasmid #34574) and subcloned into pAAV-MCS (Clontech) to generate pAAV-mArg1. Mouse arginase 1 (Arg1) shRNA sequence was cloned into the pAAV-ZsGreen-shRNA (YRGene) shuttle vector to construct pAAV-Arg1 shRNA plasmid. Adeno-associated viral particles were harvested (43).

Arginine and Ornithine Detection by LC-MS/MS. H5V cells (endothelial cell line) treated with SExos for 48 h and then arginine and ornithine level were analyzed on Ultimate 3000 rapid separation liquid chromatography coupled with TSQ Quantiva triple quadrupole mass spectrometry (MS). The MS parameters of Quantiva were described (44).

In Situ Hybridization. In situ hybridization was performed as previously described (45). Briefly, an Arg1 fragment was cloned into pGEM-T Easy vector sense and antisense probes were then generated. Cryostat sections were acetylated, permeated, prehybridized, and then incubated in hybridization buffer probes at 55 °C overnight. The sections were blocked and incubated with anti-DIG-alkaline phosphatase antibody (1:2,000) (ab119345; Abcam) in blocking buffer at 4 °C overnight. The sections then were incubated with alkaline phosphatase substrates NBT/BCIP (1383221/1383213; Roche) for appropriate time to develop the Arg1 mRNA signal. The images were captured by Spot digital camera and Leica AS LMD microscope.

Measurement of Nitrite and NO. Nitrite level in mouse aortas was measured using a Griess reagent kit (Molecular Probes). The results were presented relative to protein content. For NO measurement, human umbilical vein endothelial cells (HUVECs; Lonza) were incubated in NO-sensitive fluorescent dye 4-amino-5-methylamino-2′,7′-difluorofluorescein diacetate, and NO production was detected under a FV1000 confocal microscope (Olympus).

Statistics. Results represent means ± SEM of *n* separate experiments. Student's *t* test (two-tailed) was used when two groups were compared. One-way ANOVA followed by the Bonferroni post hoc test was used when more than two treatments were compared.

ACKNOWLEDGMENTS. We are grateful to Dr. O. J. Müller for the gift of RGDLRVS-AAV9 plasmid. This study was supported by Research Grants Council of Hong Kong (C4024-16W, T12-402/13M), National Natural Science Foundation of China (31741064, 91339117, 81471082, 81561128017), National Basic Research Program of China (2012CB517805), Beijing Natural Science Foundation (5122028), and Hong Kong Scholarship Program.

1. Théry C (2011) Exosomes: Secreted vesicles and intercellular communications. *F1000 Biol Rep* 3:15.
2. Raposo G, et al. (1996) B lymphocytes secrete antigen-presenting vesicles. *J Exp Med* 183:1161–1172.
3. Blanchard N, et al. (2002) TCR activation of human T cells induces the production of exosomes bearing the TCR/CD3/zeta complex. *J Immunol* 168:3235–3241.
4. van Niel G, et al. (2001) Intestinal epithelial cells secrete exosome-like vesicles. *Gastroenterology* 121:337–349.
5. Gajos-Michniewicz A, Duechler M, Czyz M (2014) MiRNA in melanoma-derived exosomes. *Cancer Lett* 347:29–37.
6. Conde-Vancells J, et al. (2008) Characterization and comprehensive proteome profiling of exosomes secreted by hepatocytes. *J Proteome Res* 7:5157–5166.
7. Valadi H, et al. (2007) Exosome-mediated transfer of mRNAs and microRNAs is a novel mechanism of genetic exchange between cells. *Nat Cell Biol* 9:654–659.
8. Rana S, Malinowska K, Zöller M (2013) Exosomal tumor microRNA modulates premetastatic organ cells. *Neoplasia* 15:281–295.
9. Costa-Silva B, et al. (2015) Pancreatic cancer exosomes initiate pre-metastatic niche formation in the liver. *Nat Cell Biol* 17:816–826.
10. Ghidoni R, Benussi L, Binetti G (2008) Exosomes: The Trojan horses of neurodegeneration. *Med Hypotheses* 70:1226–1227.
11. Marcilla A, et al. (2012) Extracellular vesicles from parasitic helminths contain specific excretory/secretory proteins and are internalized in intestinal host cells. *PLoS One* 7: e45974.
12. Vicencio JM, et al. (2015) Plasma exosomes protect the myocardium from ischemia-reperfusion injury. *J Am Coll Cardiol* 65:1525–1536.
13. Santovito D, et al. (2014) Plasma exosome microRNA profiling unravels a new potential modulator of adiponectin pathway in diabetes: Effect of glycemic control. *J Clin Endocrinol Metab* 99:E1681–E1685.
14. Ferrante SC, et al. (2015) Adipocyte-derived exosomal miRNAs: A novel mechanism for obesity-related disease. *Pediatr Res* 77:447–454.
15. Montezano AC, Nguyen Dinh Cat A, Rios FJ, Touyz RM (2014) Angiotensin II and vascular injury. *Curr Hypertens Rep* 16:431.
16. Valente AJ, Irimpen AM, Siebenlist U, Chandrasekar B (2014) OxLDL induces endothelial dysfunction and death via TRAF3IP2: Inhibition by HDL3 and AMPK activators. *Free Radic Biol Med* 70:117–128.
17. Chen Q, Dong L, Wang L, Kang L, Xu B (2009) Advanced glycation end products impair function of late endothelial progenitor cells through effects on protein kinase Akt and cyclooxygenase-2. *Biochem Biophys Res Commun* 381:192–197.
18. Caby MP, Lankar D, Vincendeau-Scherrer C, Raposo G, Bonnerot C (2005) Exosomal-like vesicles are present in human blood plasma. *Int Immunol* 17:879–887.
19. Al-Nedawi K, Meehan B, Kerbel RS, Allison AC, Rak J (2009) Endothelial expression of autocrine VEGF upon the uptake of tumor-derived microvesicles containing oncogenic EGFR. *Proc Natl Acad Sci USA* 106:3794–3799.
20. Simons M, Raposo G (2009) Exosomes–Vesicular carriers for intercellular communication. *Curr Opin Cell Biol* 21:575–581.
21. Morelli AE, et al. (2004) Endocytosis, intracellular sorting, and processing of exosomes by dendritic cells. *Blood* 104:3257–3266.
22. Christianson HC, Svensson KJ, van Kuppevelt TH, Li JP, Belting M (2013) Cancer cell exosomes depend on cell-surface heparan sulfate proteoglycans for their internalization and functional activity. *Proc Natl Acad Sci USA* 110:17380–17385.
23. Berkowitz DE, et al. (2003) Arginase reciprocally regulates nitric oxide synthase activity and contributes to endothelial dysfunction in aging blood vessels. *Circulation* 108:2000–2006.
24. Ryoo S, et al. (2008) Endothelial arginase II: A novel target for the treatment of atherosclerosis. *Circ Res* 102:923–932.
25. Santhanam L, et al. (2007) Inducible NO synthase dependent S-nitrosylation and activation of arginase1 contribute to age-related endothelial dysfunction. *Circ Res* 101: 692–702.
26. Katusic ZS (2007) Mechanisms of endothelial dysfunction induced by aging: Role of arginase I. *Circ Res* 101:640–641.
27. Beleznai T, Feher A, Spielvogel D, Lansman SL, Bagi Z (2011) Arginase 1 contributes to diminished coronary arteriolar dilation in patients with diabetes. *Am J Physiol Heart Circ Physiol* 300:H777–H783.
28. Romero MJ, et al. (2008) Diabetes-induced coronary vascular dysfunction involves increased arginase activity. *Circ Res* 102:95–102.
29. Mathivanan S, Fahner CJ, Reid GE, Simpson RJ (2012) ExoCarta 2012: Database of exosomal proteins, RNA and lipids. *Nucleic Acids Res* 40:D1241–D1244.
30. Zhou L, et al. (2015) Upregulation of arginase activity contributes to intracellular ROS production induced by high glucose in H9c2 cells. *Int J Clin Exp Pathol* 8:2728–2736.
31. Kashyap SR, Lara A, Zhang R, Park YM, DeFronzo RA (2008) Insulin reduces plasma arginase activity in type 2 diabetic patients. *Diabetes Care* 31:134–139.
32. Wang S, Fang F, Jin WB, Wang X, Zheng DW (2014) Assessment of serum arginase I as a type 2 diabetes mellitus diagnosis biomarker in patients. *Exp Ther Med* 8:585–590.
33. Chicoine LG, Paffett ML, Young TL, Nelin LD (2004) Arginase inhibition increases nitric oxide production in bovine pulmonary arterial endothelial cells. *Am J Physiol Lung Cell Mol Physiol* 287:L60–L68.
34. Shemyakin A, et al. (2012) Arginase inhibition improves endothelial function in patients with coronary artery disease and type 2 diabetes mellitus. *Circulation* 126: 2943–2950.
35. Ming XF, et al. (2004) Thrombin stimulates human endothelial arginase enzymatic activity via RhoA/ROCK pathway: Implications for atherosclerotic endothelial dysfunction. *Circulation* 110:3708–3714.
36. Wei SJ, et al. (2017) Poly(ADP-ribose) polymerase 1 deficiency increases nitric oxide production and attenuates aortic atherogenesis through downregulation of arginase II. *Clin Exp Pharmacol Physiol* 44:114–122.
37. Yu H, et al. (2003) Widespread expression of arginase I in mouse tissues. Biochemical and physiological implications. *J Histochem Cytochem* 51:1151–1160.
38. Royo F, et al. (2017) Hepatocyte-secreted extracellular vesicles modify blood metabolome and endothelial function by an arginase-dependent mechanism. *Sci Rep* 7:42798.
39. National Research Council (2011) Guide for the Care and Use of Laboratory Animals (National Academies Press, Washington, DC), 8th Ed.
40. Almqvist N, Lönnqvist A, Hultkrantz S, Rask C, Telemo E (2008) Serum-derived exosomes from antigen-fed mice prevent allergic sensitization in a model of allergic asthma. *Immunology* 125:21–27.
41. Tian XY, et al. (2012) Uncoupling protein-2 protects endothelial function in diet-induced obese mice. *Circ Res* 110:1211–1216.
42. Brown BD, et al. (2007) Endogenous microRNA can be broadly exploited to regulate transgene expression according to tissue, lineage and differentiation state. *Nat Biotechnol* 25:1457–1467.
43. Grieger JC, Choi VW, Samulski RJ (2006) Production and characterization of adeno-associated viral vectors. *Nat Protoc* 1:1412–1428.
44. Li X, et al. (2017) Determination of amino acids in colon cancer cells by using UHPLC-MS/MS and [U-$^{13}C_5$]-glutamine as the isotope tracer. *Talanta* 162:285–292.
45. Obernosterer G, et al. (2007) Locked nucleic acid-based in situ detection of microRNAs in mouse tissue sections. *Nat Protoc* 2:1508–1514.